

Estradiol Valerate Determination in Whole-Blood Samples using FFT Square Wave Voltammetry and Supported Liquid Membrane Micro-Extraction

Mahboubeh Morshedi¹, Zahra Mofidi¹, Parviz Norouzi^{1,2,*}, Bagher Larijani³, Shirin Shahabi¹

¹ Center of Excellence in Electrochemistry, School of Chemistry, College of Science, University of Tehran, Tehran, Iran

² Biosensor Research Center, Endocrinology & Metabolism Molecular-Cellular Sciences Institute, Tehran University of Medical Sciences, Tehran, Iran

³ Diabetes Research Center, Endocrinology & Metabolism Research Institute, Tehran University of Medical Sciences, Tehran, Iran

*E-mail: norouzi@khayam.ut.ac.ir

Received: 31 July 2018 / Accepted: 20 September 2018 / Published: 1 October 2018

Herein, a new analytical technique based on fast Fourier transmission square wave voltammetry (FFTSWV) coupled with Flat Sheet Supported Liquid Membrane (FSSLM) was used for the extraction and subsequent determination of estradiol valerate (EV) in whole blood samples. First, EV was extracted from the blood sample through a PTFE membrane soaked in 1-octanol into a buffer solution, and then it was oxidized on a carbon paste electrode modified with cerium carbonate nanospheres. The effect of different separation parameters such as membrane solvent, pH of donor and acceptor phases, and extraction time on the recovery of EV was investigated. This coupled technique showed two linear calibration regions. Based on the first calibration region (10–500 ng mL⁻¹), the detection limit of the method was 2 ng mL⁻¹ with R-square of 0.995. Under the optimal conditions, EV was effectively extracted from the whole blood sample with recovery percentage of 52% and pre-concentration factor of 1.5. Considering the complex media of the blood sample, this assay can be a competitive analytical method for the determination of EV in complex samples like blood.

Keywords: Estradiol valerate, Supported Liquid Membrane, FFT Voltammetry, Extraction

1. INTRODUCTION

One of female Steroid hormones is Estradiol valerate which belongs to the grouping of Endocrine disrupting chemicals (EDCs) [1]. EDCs disrupt endocrine systems through mimicking hormonal interactions, which may practically cause metabolic abnormalities and human carcinogenesis such as

testicular, prostate, and ovarian cancers [2]. Nowadays, the ubiquitous usage of EDCs in packaging industries, pesticides, animal food, and human food has triggered intense medical concern as well as several regulations on the highly permitted level of EDCs in foods and water have been exerted [3, 4]. Among EDCs, the trace determination of EV in the biological samples such as blood and urine is highly significant as its enhanced level can result in several medical diseases such as uterine pathology and breast cancer [5, 6]. Fig. 1 illustrates the chemical structure of EV.

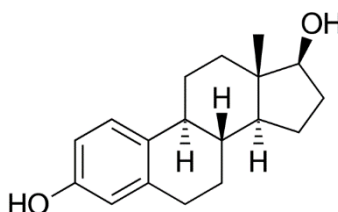


Figure 1. Chemical structure of EV molecule

The EV analysis in some real samples such as food and blood is not easy due to their complex environments and matrices probable interference. Up to now, the majority of the quantitative analyses of EV have been performed in environmental water matrices [7-10]. High Performance Liquid Chromatography (HPLC) [11-13] Gas Chromatography (GC) [14] and Mass Spectroscopy (MS) [15] can be implied as the conventional methods that have been employed for their analysis. Normally, a sample preparation method like Liquid–Liquid Extraction (LLE) [16] and Solid Phase Extraction (SPE) [17] could be conducted before the determination step to clean matrices impact of the real sample. Since most of the preparation methods need high volumes of toxic organic solvents, some new methods such as Solid Phase Microextraction (SPME) [18] have been developed, which also has created the chance for automation [19]. Nevertheless, while using SPME has opened up a new path for quantitative analysis of biological compounds, there are still some challenges like fiber fragility as well as robustness in contact with the specimens.

Another sample preparation method is Supported Liquid Membrane (SLM) which also needs less organic volume [20]. Compared with the mentioned techniques, it is simple, comparatively stable, user-friendly, and low-cost as well. A small amount of organic solvent, in the present method, was held within the pores of a polymeric membrane, separates two aqueous phases [21]. Passive diffusion from the donor phase to the acceptor phase [22] is the mechanism of the transport. There are various kinds of SLM based on size and shape, among which Flat Sheet Supported Liquid Membrane (FSSLM) is the simplest and therefore has received intense interest [23, 24].

Recent reports illustrate that by Fast Fourier Transmission Voltammetric techniques, it could be possible to measure sub-nanomolar amounts of pharmaceuticals in complex matrixes, which indicates their potential applicability as a highly sensitive electrochemical method [25-27]. Voltammetric and background signal in this technique, are transformed to frequency domain and resolved for the background interference using a discrete Fast Fourier Transformation (FFT). As a result, the integration of FFT into the conventional SWV can represent a more sensitive electrochemical measurement.

In this case, to determine EV, a novel electroanalytical technique, based on the coupling of FSSLM and FFTSWV techniques together is used. The process of extraction and following the determination is carried out in a single separation cell. In addition, with no specific pretreatment, the blood sample is directly injected into the separation cell and monitored for the next steps. .

2.1. Materials and reagents

PTFE membrane was purchased from the German Membrane Company. EV was purchased from Aburaihan Pharmaceutical Co. (Tehran, Iran). 1-Octanol (99%), Dioctyl Phthalate (DOP) (99.5%), Dibutyl Phthalate (DBP) (99.5%), Propanol (99%), Graphite powder, Sodium Carbonate (99%), Cerium chloride (99.5%), Orthophosphoric acid (85%, w/w), sodium hydroxide (98%) and ethanol (96%) were provided from Merck (Darmstadt, Germany) in analytical grades.

2.2. Preparation of the $Ce_2(CO_3)_3$ nano-particle-modified electrode

First, $Ce_2(CO_3)_3$ nanoparticles were synthesized according to a previous method [28]. Briefly, two solutions of 10 mM Sodium carbonate and 50 mM Cerium chloride were prepared. The Cerium solution was introduced into the Carbonate solution with a feed flow rate of 10 mL min⁻¹ using a peristaltic pump at room temperature. After the feeding was completed, the Cerium carbonate precipitate was collected and washed three times with water and ethanol, and then dried in oven at 80 °C for 8 hrs. Finally, for the preparation of CPE, the $CeCO_3$ nanoparticles were mixed with graphite powder, and paraffin in weight ratio of 5 : 75 : 20. Then, it was pasted and pressed into a syringe.

2.3. Biological sample preparation

A stock solution of EV analyte with a concentration of 50 mg mL⁻¹ was prepared in ultrapure ethanol, and then it was sealed and stored at 4 °C. All other Sample solutions were prepared from this stock solution by dilution with Phosphate Buffer Solution (PBS), every day. The whole blood samples, obtained from Iranian Blood Transfusion Organization, used as match matrix to generate the calibration curve, and they were stored at 4 °C before their analysis. The whole blood samples were diluted with a ratio of 1:3 by doubly distilled water and their pH values adjusted to 7.0. These sample solutions were used in the FSSLM-FFTSWV without any sample pretreatment.

2.4. The electrochemical Setup

Fig. 2 shows a schematic diagram of the separation cell and electrochemical setup. The separation cell includes a donor phase, a PTFE membrane, and an acceptor phase. The membrane is immersed in an organic solvent for 1 hour before it is applied to the separation cell. The volume of donor phase and acceptor phase is 12 mL and 4 mL in all experiments, respectively.

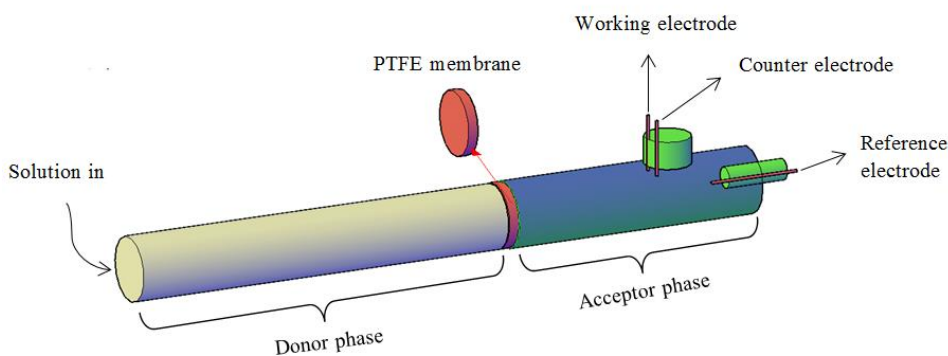


Figure 2. Schematic diagram of the separation cell and the electrochemical setup

2.5. The electrochemical detection technique

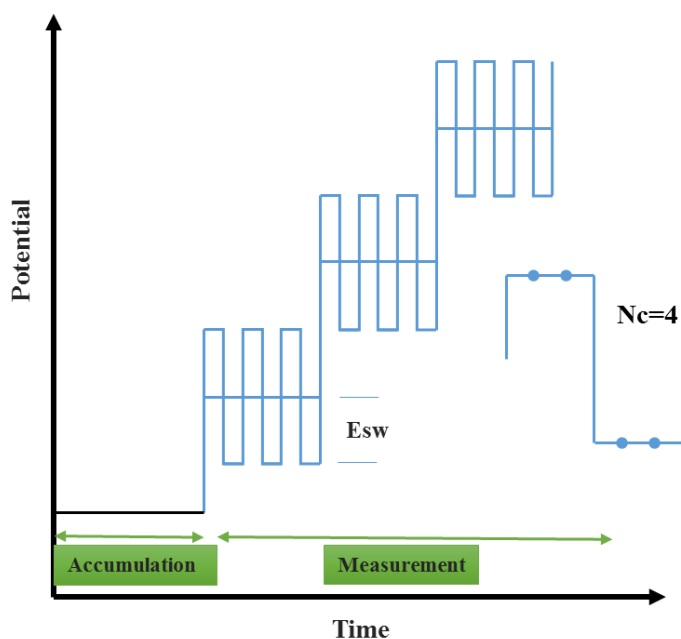


Figure 3. The diagram of the potential waveform used in measurements

The FFTSW voltammetric experiments were accomplished using a potentiostat connected to a PC PIV with an A/D board (PCL-818H, Advantech Co.). The voltammetric system was controlled using a Delphi 6.0-based software capable of applying analog waveforms to the WE and receiving and recording the current responses from the data acquisition board [29]. The measurements were performed under cyclic voltammetry (CV) and FFTSWV modes. The potential excitation waveform which was used to enhance the sensitivity of the method is illustrated in Fig. 3. This waveform is composed of accumulation (a) and measurement (b) sections. The former involves applying an accumulation potential (E_s) of -1000 mV for 2s to the WE and is followed by the measurement part, where the waveform involves applying multiple SW pulses with an amplitude and frequency of E_{sw} and f_0 (Fig 3.) to the staircase potential function. The staircase potential is altered by small potential steps (ΔE). The current was sampled 4 times at each SW pulse cycle.

2.6. Calculation of preconcentration factor, extraction recovery, relative recovery, and relative error

The preconcentration factor (PF) is defined as the ratio between the final analyte concentration in the acceptor phase ($C_{f,a}$) and the initial concentration of analyte ($C_{i,s}$) in the donor phase solution:

$$PF = \frac{C_{f,a}}{C_{i,s}} \quad (1)$$

$C_{f,a}$ is calculated based on a calibration curve obtained from direct electrochemical measurement of standard analyte solutions.

The extraction recovery (ER %) is defined as the ratio of the extracted moles of analyte in the acceptor phase to those initially existed in the donor phase:

$$ER\% = \frac{V_{f,a}}{V_{i,s}} PF \times 100 \quad (2)$$

$V_{f,a}$ and $V_{i,s}$ are the volumes of the acceptor phase and the sample solution, respectively. Relative recovery is calculated according to the following equation:

$$RR\% = \frac{C_{found} - C_{real}}{C_{added}} \times 100 \quad (3)$$

C_{found} , C_{real} , and C_{added} are the analyte concentration determined after a known amount added to the real sample, the initial concentration of the analyte in the real sample, and the known amount of spiked concentration.

3. RESULTS AND DISCUSSION

3.1. Surface characterization of $Ce_2(CO_3)_3$ nano-particle modified CPE

Fig. 4 a and b shows FESEM images of $Ce_2(CO_3)_3$ nanostructure powder and $Ce_2(CO_3)_3$ -modified carbon paste. In Fig. 4, a cerium carbonate nanoparticles show a sphere-like morphology whose sizes are between 50 nm to 100 nm. Furthermore, the interconnected particles constitute a highly porous surface structure which can expose more active sites of cerium carbonate to the solution, for EV oxidation. In Fig. 4b, Cerium carbonate nanoparticles have been incorporated on the surface of graphite sheets, which enhances the conductivity of the cerium carbonate and its efficient utilization.

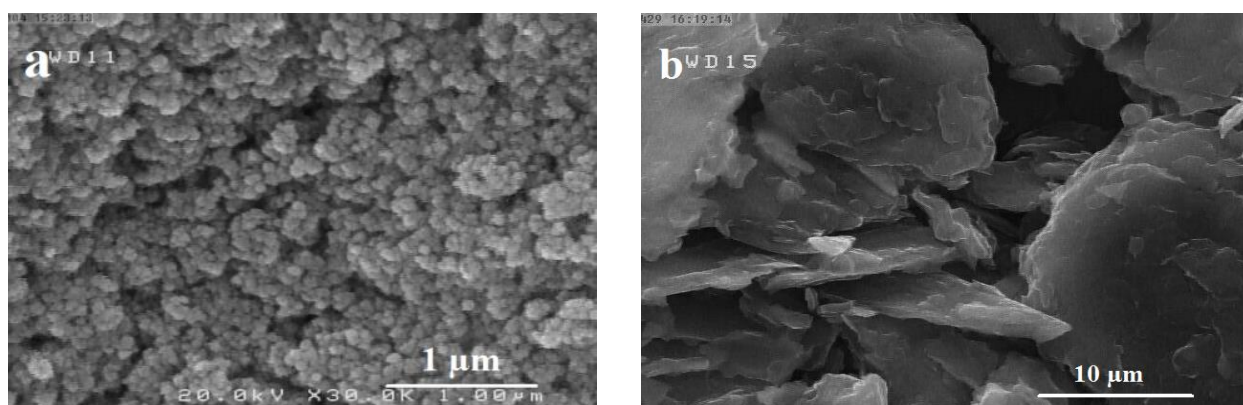


Figure 4. FESEM image of nanosphere-like particles of (a) $Ce_2(CO_3)_3$ and (b) $Ce_2(CO_3)_3$ -modified carbon paste

3.2. Electrochemical behavior study

Fig. 5a shows the cyclic voltammograms of $\text{Ce}_2(\text{CO}_3)_3$ -modified CPE in buffer solution without EV and also $2.7 \mu\text{g mL}^{-1}$ EV on the bare CPE and $\text{Ce}_2(\text{CO}_3)_3$ -modified CPE. Comparing recorded CVs for the redox reaction of the analyte, the peak current at the modified CPE, with a small negative potential shift, is larger than the obtained peak current at bare CPE, which is an indication of the electrocatalytic oxidation of EV by Cerium carbonate. Fig. 5b shows the effect of the change in mass percentages of Cerium carbonate in the CPE composition in the range of 0 to 10% on the peak currents, at a scan rate of 100 mV s^{-1} . As shown, the current signal increases with Cerium carbonate percentage up to 5%, but higher than that value the peak current weakens. This effect could be due to the low conductivity of the Cerium carbonate which reduces the conductivity of the CPE medium when it is used at high amounts.

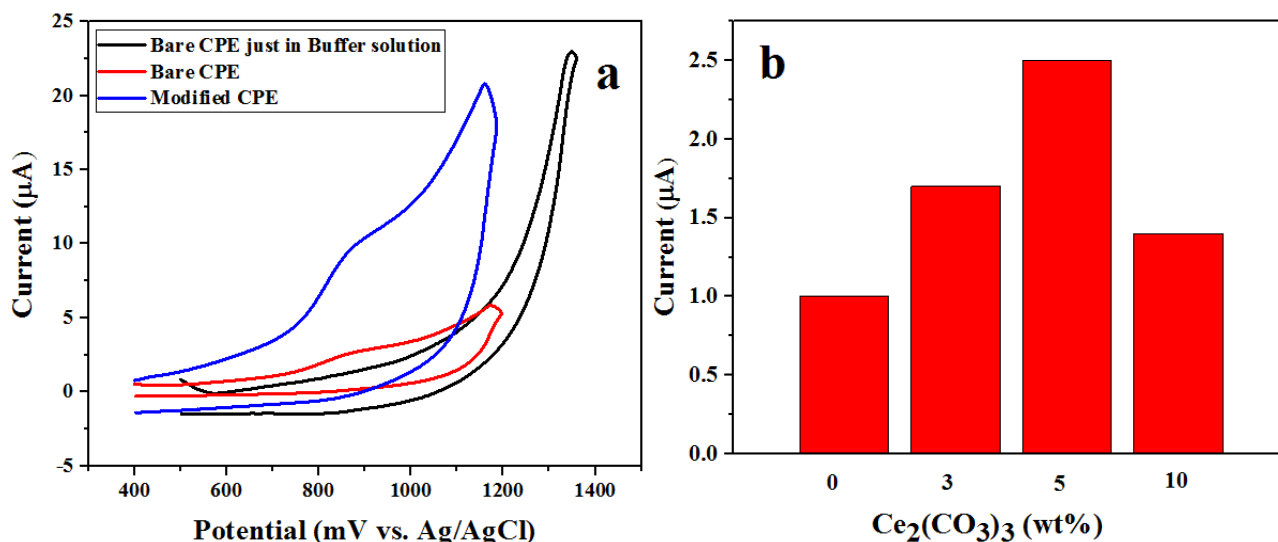


Figure 5. (a) Cyclic voltammograms of (a) $\text{Ce}_2(\text{CO}_3)_3$ -modified CPE in buffer solution, and Cyclic voltammograms of $\text{Ce}_2(\text{CO}_3)_3$ -modified CPE and bare CPE in buffer solution containing $2.7 \mu\text{g mL}^{-1}$ EV at 500 mV s^{-1} and $\text{pH} = 7$. (b) The effect of different weight percentages of cerium carbonate in the carbon paste electrode on the EV currents at scan rate of 100 mV s^{-1} and concentration of $2.7 \mu\text{g mL}^{-1}$.

3.2.1. FFTSWV parameters optimization

Frequency and amplitude are two important variables in FFTSWV, since the signal of the analyte, background noise, and peak shape depends on condition of the excitation signal. The FFTSWV of $2.7 \mu\text{g mL}^{-1}$ EV in phosphate buffer $\text{pH} 7$ were investigated within the frequency range of 88-11300 Hz, amplitude 5 to 200 mV and four cycles. A plot of SW frequency and amplitude versus current (Fig.6) showed that the maximum current was achieved by applying a frequency of 11300 Hz and an amplitude of 50 mV.

As shown in the Fig. 6, the SW peak currents increase with increasing the SW frequency up to 11300 Hz and then decreased. This can be due to the fact that the SW frequency acts similar to sweep

rate in cyclic voltammetry. Therefore, at SW frequencies lower than 5670 Hz the response values are low.

Fig. 6 also depicts the influence of SW amplitude on the electrode response. As can be seen, the electrode response is increased with amplitude increasing up to 50 mV, which may be attributed to the fast excitation and higher diffusion rate of the analyte. However, at higher amplitude values, a decline is observed in the electrode response due to the kinetic limitation. Consequently, based on the results, the optimum values for FFTSWV determination of EV were frequency of 11300 and amplitude 50 mV.

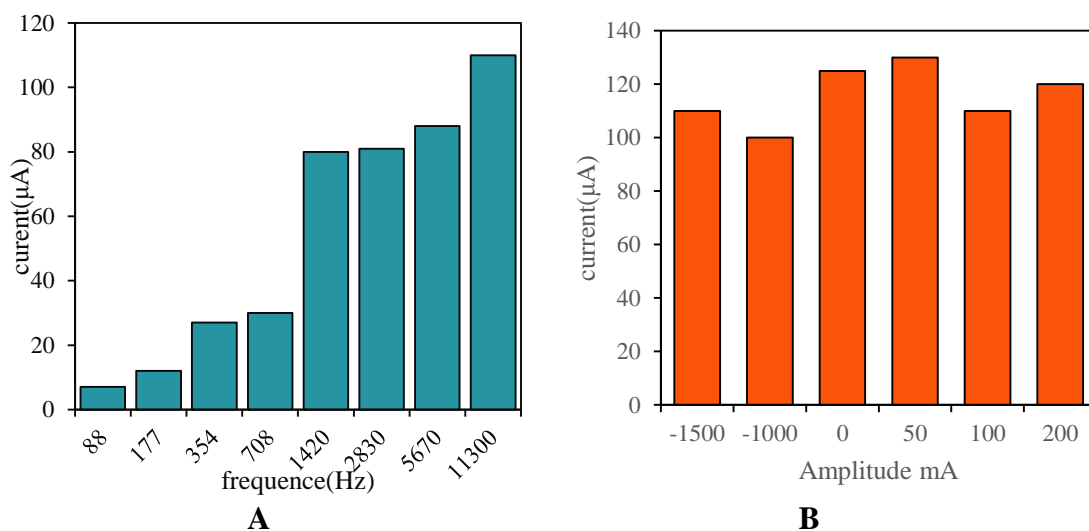


Figure 6. The effect of frequency and amplitude on the response of CPE with 0.5 $\mu\text{g/mL}$ EV in 0.1 M phosphate buffer pH 7

3.3. Effective parameters on the extraction recoveries of EV

Figs. 7 a to c show the impact of various parameters on the extraction recoveries of EV in the separation cell. Fig. 8a illustrates the dependence of the extraction recovery on the solvent type used in the membrane. The result indicates that highest and the lowest extraction recoveries belong to 1-Octanol and toluene, respectively. This behavior suggests that the protic and polar solvent could assist the EV transport across the membrane, probably via its hydrogen bonding ability with EV. Furthermore, the electrochemical measurement data, in the acceptor phase, shows that a larger electrode signal is obtained when 1-octanol was used in the membrane compared with when 1-propanol, DBP, and DOP were used.

Fig. 7b shows a 3D plot of acceptor/donor pH effect on the extraction recovery. This pH effect could be explained as following; increasing the pH promotes deprotonation of EV hydroxyl groups which is suitable for the oxidative reaction in a voltammetric scan. Nevertheless, with increasing the pH higher than 7.0 other parameters such as phase emulsification [1] or membrane/electrode effects set in. Therefore, an optimum pH of 7.0 was selected for the acceptor phase. The other dimensions of the plot shows the effect of the pH of donor phase on the extraction recovery when the pH of acceptor phase is kept at 7.0. The observed pattern pinpoints the importance of keeping a pH difference between the two phases, as it is a requirement for analyte transport [30]. Based on the obtained curve, the pH of the donor phase selected to be 2.0.

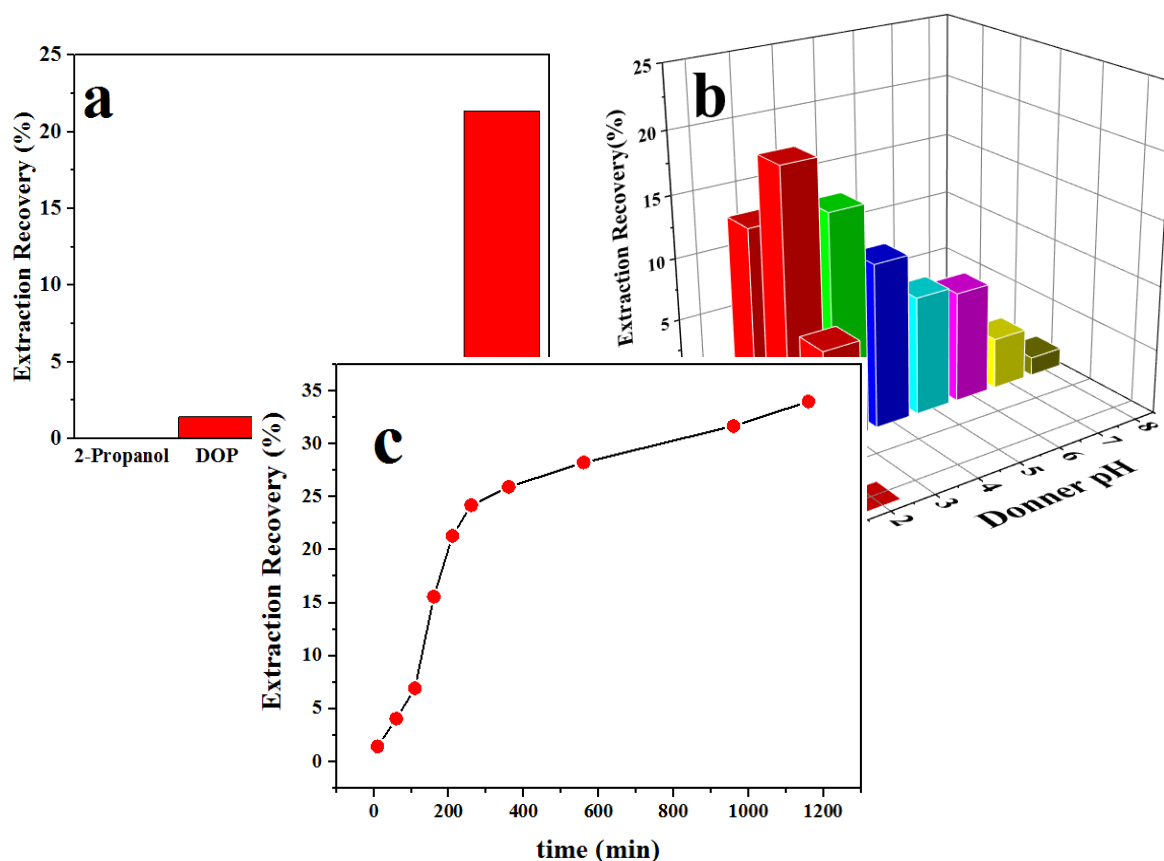


Figure 7. The effect of different parameters on the Extraction Recovery based on the FFTSWV (a) The effect of solvent type used in the separation membrane (b) pH of acceptor/donor phase, and c extraction time on the extraction recovery of EV

Fig. 7c shows the effect of extraction time on the recovery percentages obtained from different FFTSWV currents. At first, the electrode response increases sharply, which may be due to abundant sites on the membrane through which EV can transport, but after 180 minutes, only a slight enhancement in the response is observed, suggesting that the membrane sites for EV transport are saturated. This result implies that the best extraction time for the analyte is 180 minutes.

3.4. The analytical performance

Finally, EV was measured in the in Blood as real sample by the FFTSWV technique. To obtain the calibration curve, different concentrations of EV were spiked into blood sample kept in the donor phase, and their FFTSWV responses were measured. As shown in Fig. 8, there are two concentration ranges for the calibration curves, with good correlation coefficient factors of 0.99044 and 0.99503 for the first and the second curves, respectively. The calibration curve at the concentrations range is more sensitive due to the abundant transport paths in the membrane. In that concentration range, also, there is more active sites on the $\text{Ce}_2(\text{CO}_3)_3$ -modified CPE surface, which may facilitate oxidation of EV, may become saturated at high concentration of EV.

Table 1. Figures of merit for the determination of EV using FSSLM-FFTSWV technique.

	LOD*	LOQ*	L.R.*	RSD(%)
Calibration curve 1	2	7	10 - 500	7.1%
Calibration curve 2	-	-	500– 5000	7.1%

* Quantities are in ng mL⁻¹

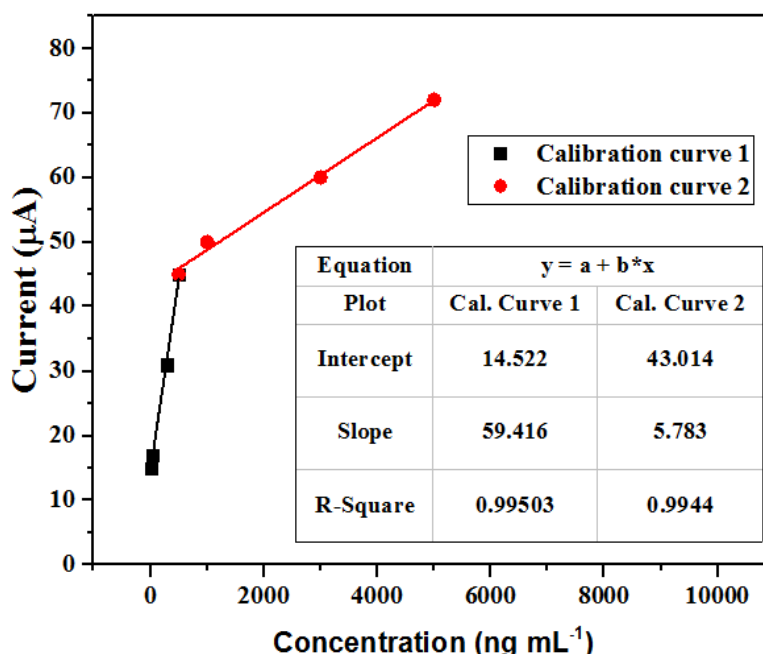


Figure 8. Calibration curves obtained based on different spiked concentrations of EV into blood sample.

The first calibration curve shows a linear range (L.R.) of 10 - 500 ng mL⁻¹, and the second calibration curve shows an L.R. of 500 – 5000 ng mL⁻¹. Furthermore, based on practical experiments, LOD value was achieved. To that end, the analyte concentration was decreased till the EME-FFTSWV response of EV showed detectable signals-to-noise ratio of 3 (3S/N). The lowest concentrations from which the linearity of the calibration curve was started from it considered LOQ. Under the optimal conditions, EV was effectively extracted from the whole blood sample with recovery percentage of 52% and pre-concentration factor of 1.5. The figures of merits are shown in Table 1.

3.5. Analysis of real samples

In order to show the applicability of the FSSLM-FFTSWV method a whole blood sample was analyzed using this technique. The results are presented in Table 2. To determine the method accuracy, an exact amount of EV was spiked in the whole blood sample and the procedure was performed to calculate the relative recovery (RR%) and error according to equation 3. The RR%, Error%, and RSD%

of the method were 92.6, 7.3%, and 5.3%, respectively. These results verify robustness of the FSSLM-FFTSWV for determination of EV in whole blood samples.

Table 2. Determination of EV in whole blood samples using FSSLM-FFTSWV

Blood Sample	C_{real} (ng mL ⁻¹)	ND ^a
	C_{add} (ng mL ⁻¹)	300
	C_{found} (ng mL ⁻¹)	278
	RR%	92.6
	Error%	7.3
	RSD%	5.3

^a ND: not detected

Table 3. A comparison of the FSSLM-FFTSWV technique with previous techniques reported for the determination of EV.

Method	Sample	LOD*	L.R.*	Ref.
Fe ₃ O ₄ -MIP	River water	5.45	13.6 to 2723.8	[1]
Cu-BTC frameworks-sensitized electrode	Environmental water	0.33	–	[30]
HPLC-UV	Aqueous Tea	2.8–7.1	–	[31]
LL Microextraction	Human Urine	250	(1 to 250) × 10 ³	[32]
FSSLM-FFTSWV	Blood	2.00	10 to 500	This work

*quantities are in ng mL⁻¹

Table 3 compares the LOD and L.R. of the present technique and analytical techniques reported in the literature for the determination of EV. The LOD and L.R. of the FSSLM-FFTSWV technique is 2, and 20-500 ng mL⁻¹, respectively. Regarding the complex matrices of blood compared with other samples, the figures of merit are better than the previously reported measurement assays for EV, suggesting the competitiveness of the present method for complex media analysis.

4. CONCLUSION

In the present paper, FFTSWV and FSSLM techniques were combined to be proposed as a new method for the extraction and determination of EV in blood samples. Initially, EV was extracted to the

receiver phase and then was oxidized on the surface of a cerium carbonate-modified CPE by FFTSWV. Using FFTSWV method beside the suitable modifier led to the novel and sensitive method for EV determination due to having excellent improvement in S/N ratio. The introduced method was adequately applicable for highly selective and sensitive detection of EV at low concentrations. Furthermore, the prepared assay showed acceptable potential to be competitive with other analytical methods applied for the determination of EV and other probable Estroides in complex matrices such as blood samples.

ACKNOWLEDGEMENT

The authors thanks the research council of University of Tehran for the financial support of this work.

References

1. A.A. Lahcen, A.A. Baleg, P. Baker, E. Iwuoha and A. Amine, *Sens. Actuators B*, 241 (2017) 698.
2. P.M. Ndagili, A.M. Jijana, P.G. Baker and E.I. Iwuoha, *J. Electroanal. Chem.*, 653 (2011) 67.
3. Y. Hao, R. Gao, L. Shi, D. Liu, Y. Tang and Z. Guo, *J. Chromatogr. A*, 1396 (2015) 7.
4. Q. Han, X. Shen, W. Zhu, C. Zhu, X. Zhou and H. Jiang, *Biosens. Bioelectron.*, 79 (2016) 180.
5. J.F. Dorgan, F.Z. Stanczyk, L.L. Kahle and L.A. Brinton, *Br. Canc. Res.*, 12 (2010) R98.
6. M. Morelli, A. Sacchinelli, R. Venturella, R. Mocciaro and F. Zullo, *J. Obst. Gyn. Res.*, 39 (2013) 985.
7. W. Gao, T. Stalder and C. Kirschbaum, *Talanta*, 143 (2015) 353.
8. T. Vega-Morales, Z. Sosa-Ferrera and J. Santana-Rodríguez, *J. Hazard. Mater.*, 183 (2010) 701.
9. F.C. Moraes, B. Rossi, M.C. Donatoni, K.T. de Oliveira and E.C. Pereira, *Anal. Chim. Acta*, 881 (2015) 37.
10. L. Yuan, J. Zhang, P. Zhou, J. Chen, R. Wang, T. Wen, Y. Li, X. Zhou and H. Jiang, *Biosens. Bioelectron.*, 29 (2011) 29.
11. S. Poschner, M. Zehl, A. Maier-Salamon and W. Jäger, *J. Pharm. Biomed. Anal.*, 138 (2017) 344.
12. S. Szarka, V. Nguyen, L. Prokai and K. Prokai-Tatrai, *Anal. Bioanal. Chem.*, 405 (2013) 3399.
13. B. Ebrahimpour, Y. Yamini, S. Seidi and F. Rezaei, *Anal. Meth.*, 6 (2014) 2936.
14. B. Yilmaz, *Anal. Sci.*, 26 (2010) 391.
15. N. Krone, B.A. Hughes, G.G. Lavery, P.M. Stewart, W. Arlt and C.H. Shackleton, *J. Ster. Biochem. Mol. Biol.*, 121 (2010) 496.
16. L. Vidal, M.-L. Riekkola and A. Canals, *Anal. Chimica. Acta*, 715 (2012) 19.
17. J. Ding, Q. Gao, X.S. Li, W. Huang, Z.G. Shi and Y.Q. Feng, *J. Sep. Sci.*, 34 (2011) 2498.
18. Y. Hu, Y. Wang, X. Chen, Y. Hu and G. Li, *Talanta*, 80 (2010) 2099.
19. R.L. Pérez and G.M. Escandar, *Microchem. J.*, 118 (2015) 141.
20. Z. Mofidi, P. Norouzi, S. Seidi and M.R. Ganjali, *New J. Chem.*, 41 (2017) 13567.
21. L. Lozano, C. Godínez, A. De Los Rios, F. Hernández-Fernández, S. Sánchez-Segado and F.J. Alguacil, *J. Mem. Sci.*, 376 (2011) 1.
22. M. Eskandari, Y. Yamini, L. Fotouhi and S. Seidi, *J. Pharm. Biomed. Anal.*, 54 (2011) 1173.
23. A. Surucu, V. Eyupoglu and O. Tutkun, *J. Industr. Eng. Chem.*, 18 (2012) 629.
24. Z. Mofidi, P. Norouzi, S. Seidi and M.R. Ganjali, *Anal. Chim. Acta*, 972 (2017) 38.
25. P. Norouzi, M.R. Ganjali, P. Daneshgar, T. Alizadeh and A. Mohammadi, *Anal. Biochem.*, 360 (2007) 175.
26. P. Norouzi, F. Faridbod, B. Larijani and M.R. Ganjali, *Int. J. Electrochem. Sci.*, 5 (2010) 1213.
27. G.N. Bidhendi, P. Norouzi, P. Daneshgar and M.R. Ganjali, *Int. J. Electrochem. Sci.*, 5 (2010) 1213.
28. A. Baranski and A. Szulborska, *J. Electroanal. Chem.*, 373 (1994) 157.

29. D.B. A. Neplenbroek and C. Smolders, *J. Memb. Sci.*, 67 (1992) 133.
30. L. Ji, Y. Wang, K. Wu and W. Zhang, *Talanta*, 159 (2016) 215.
31. P.-S. Cai, D. Li, J. Chen, C.-M. Xiong and J.-L. Ruan, *Food Chem.*, 173 (2015) 1158.
32. K.R. E. Kupcová, *J. Sep. Sci.*, 12 (2017) 2620.

© 2018 The Authors. Published by ESG (www.electrochemsci.org). This article is an open access article distributed under the terms and conditions of the Creative Commons Attribution license (<http://creativecommons.org/licenses/by/4.0/>).